Estuarine, Coastal and Shelf Science 259 (2021) 107476

Contents lists available at ScienceDirect

Estuarine, Coastal and Shelf Science

journal homepage: www.elsevier.com/locate/ecss

Land-based sediment sources and transport to southwest Puerto Rico coral reefs after Hurricane Maria, May 2017 to June 2018

Renee K. Takesue [a,*], Clark Sherman [b], Natalia I. Ramirez [b], Aaron O. Reyes [c], Olivia M. Cheriton [a], Roberto Viqueira Ríos [d], Curt D. Storlazzi [a]

[a] U.S. Geological Survey, Pacific Coastal and Marine Science Center, 2885 Mission Street, Santa Cruz, CA, 95060, USA
[b] University of Puerto Rico at Mayagüez, Dept. Marine Sciences, P.O. Box 9000, Mayagüez, PR, 00681, USA
[c] Westfield State University, Chemical and Physical Sciences, 577 Western Avenue, Westfield, MA, 01086, USA
[d] Protectores de Cuencas, Inc., P.O. Box 1563, Yauco, PR, 00698, USA

ARTICLE INFO

Keywords:
Guánica
Puerto Rico
Runoff
Geochemistry
Hurricane
Coral reef

ABSTRACT

The effects of runoff from land on nearshore ecosystems, including coral reef communities, are influenced by both sediment supply and removal by coastal processes. Integrated studies across the land-sea interface describing sources and transport of terrestrial sediment and its nearshore fate allow reef protection initiatives to target key onshore and offshore areas. Geochemical signatures in the fine fraction of terrestrial sediment from watersheds in southwest Puerto Rico were determined by multivariate principal component analysis and used to identify terrestrial sources of sediment runoff to nearshore coral reefs. Sediment settling out of suspension at reefs was collected at approximately 2 month-long intervals in bottom-mounted sediment traps from May 2017 to June 2018, a period that included Hurricanes Irma and Maria. Bulk sediment accumulation rates in traps exceeded a 10 mg/cm^2/d threshold found to stress corals at 5 of 7 reef sites throughout the 13 month-long study. Geochemical signatures showed that watersheds 10s km to the east were a predominant, year-round source of fine sediment to reefs offshore of Guánica Bay and could have introduced sediment-bound contaminants due to a higher degree of industrialization and urbanization than the local watershed. Sediment runoff from the local watershed appeared to be constrained to a narrow band close to shore. During the 2.5 months after Hurricanes Irma and Maria, bulk sediment accumulation rates increased substantially and fine sediment geochemical signatures were indicative of predominantly distal sources, except outside of the mouth of Guánica Bay, which was strongly impacted by local runoff. Mass wasting, sediment runoff, and coastal turbidity persisted for months after Hurricane Maria and could account for the appearance of a small fraction of geochemical variance from a distal sediment source that appeared in reef traps 4 months post-hurricane and persisted through the end of the study 9 months post-hurricane. Sediment geochemical sourcing in temporally resolved records from sediment traps showed how landscape-scale changes after a major hurricane affected both near-term and long-term sediment delivery to reef communities. In addition, the importance of fine sediment advection from distal sources indicates that successful reduction of land-based pressures on nearshore ecosystems will require cross-jurisdictional strategies.

1. Introduction

Healthy coastal ecosystems support a diversity of species, protect shorelines from storms, attract economic opportunities, and have aesthetic and cultural value (Carriger et al., 2013; Costanza et al., 2014; Spalding et al., 2013; Storlazzi et al., 2019). Such traits also lead to growth of population centers whose material needs alter landscapes, material flows, and physical and biogeochemical processes in ways that can compromise ecological integrity (e.g., Day et al., 2016; Duarte, 2009; Meybeck and Vorosmarty, 2005; Syvitski et al., 2005; Waterhouse et al., 2016; Wong et al., 2014). An integrated understanding of spatial and temporal scales of many processes is essential for successful mitigation of anthropogenic pressures on coastal ecosystems because impact mechanisms may not coincide in space or time and may cross geographic and jurisdictional boundaries (Alvarez-Romero et al., 2015; Newton et al., 2012; Smith et al., 2011). At developed coasts, for example,

* Corresponding author.
E-mail address: rtakesue@usgs.gov (R.K. Takesue).

https://doi.org/10.1016/j.ecss.2021.107476
Received 15 December 2020; Received in revised form 9 June 2021; Accepted 14 June 2021
Available online 18 June 2021

sediment and contaminant pressures associated with point and non-point source agricultural, municipal, and industrial waste streams can be chronic (Kroon et al., 2014; Larsen and Webb, 2009; Orth et al., 2010), and sediment removal from nearshore regions tends to occur seasonally or intermittently during storms by processes that are not under human control (DeMartini et al., 2013; Draut et al., 2009; Lugo-Fernández et al., 1994; Storlazzi et al., 2009). By coupling restoration, conservation, and management activities in watersheds and nearshore regions with the spatial and temporal scales of coastal processes, efforts can more effectively target key sites and ecologically relevant periods (Brodie and Pearson, 2016; Newton et al., 2012).

Runoff of land-derived, or terrigenous, sediment and contaminants is a pervasive threat to coastal ecosystems, including shallow coral reefs (Bartley et al., 2014; Fabricius, 2005; Orlando and Yee, 2017; Restrepo et al., 2006). Unlike material delivered episodically during storms, point and non-point source runoff can occur year-round, increasing the susceptibility of corals to other stressors such as disease, competition, and temperature (e.g., Acevedo et al., 1989; Fabricius, 2005; Rogers, 1990; Weiss and Goddard, 1977). Strategies for protecting coastal ecosystems from runoff include impoundment, modification of land use, reconnection of natural drainage pathways and sediment storage features, and revegetation—all of which rely on knowledge about runoff-producing areas (Poleto et al., 2009; Ramos-Scharron et al., 2015). One way to link runoff to its origin on the landscape is by using geochemical signatures in sediment conferred by parent rock lithologies (e.g., Anderson et al., 2018; Araújo et al., 2002; Gellis and Mukundan, 2013; Rosenbauer et al., 2013; Takesue and Storlazzi, 2017).

An integrated oceanographic, sediment trap, and geochemical study was undertaken in a sediment-impacted Caribbean coral reef ecosystem in order to characterize current sources of land-derived sediment, its nearshore fate, and implications for local watershed restoration initiatives aimed at reducing runoff. One poorly understood aspect of reef protection is the role of terrigenous sediment advected from distal watersheds (Hernandez et al., 2009; Otero and Carbery, 2005; Warne et al., 2005), which the spatial and temporal information from sediment traps can help address. Hurricanes Irma and Maria occurred during the trap deployment and the resulting sediment and geochemical time series provide insights about long-term impacts of storm-related watershed runoff and sediment delivery to nearshore coral reefs.

2. Site description

Coral reef ecosystems on the insular shelf offshore and west of Guánica Bay in southwest Puerto Rico are among the most diverse on the island, but are increasingly threatened by runoff of sediment and contaminants from coastal watersheds (Acevedo et al., 1989; García-Sais et al., 2008; Pait et al., 2008a; Ryan et al., 2008; Warne et al., 2005; Whitall et al., 2014). Guánica Bay and the Río Loco watershed were identified by the U.S. Coral Reef Task Force as a priority location for watershed initiatives to reduce impacts of anthropogenic runoff to nearby coral reef ecosystems (Whitall et al., 2013). As part of a baseline assessment for restoration activities, a 2009–2012 sediment trap time series with near-monthly resolution showed that Guánica Bay was an effective sink for terrigenous sediment, attenuating more than 50% of the signal (Sherman et al., 2013). On the reef platform offshore and west of Guánica Bay, overall sediment accumulation rates reflect regional hydrographic processes, particularly bottom sediment resuspension by waves (Hernandez et al., 2009; Sherman et al., 2013).

The current study spans the land-sea boundary from south-facing uplands of the western and central volcanic provinces to the insular shelf of Puerto Rico (Fig. 1 inset). The rocks underlying the study area contain a longitudinally sequential lithologic and geochemical record of island-arc evolution, from primitive tholeiitic basalt in the west to intermediate potassium-rich calc-alkaline andesite in the east (Jolly et al.,

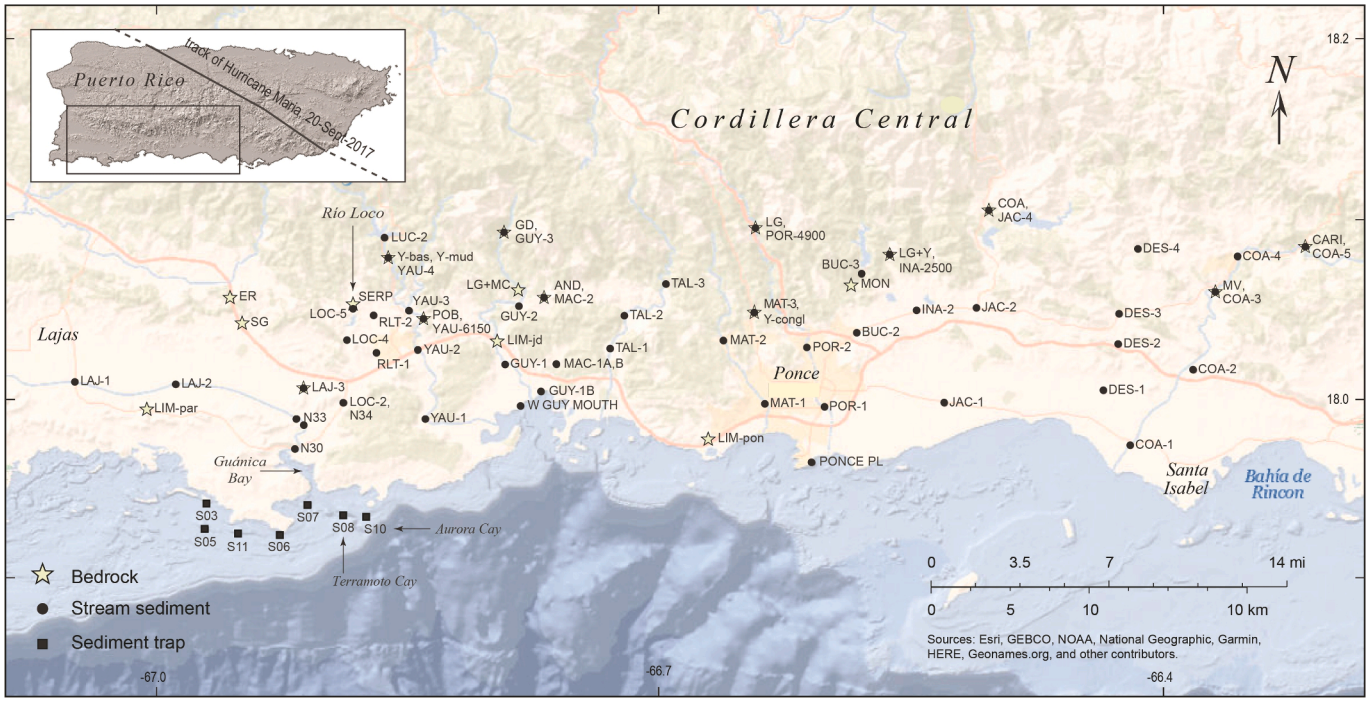

Fig. 1. Hillshade and bathymetry maps annotated with collection sites for bedrock (stars), stream sediment (circles), and sediment traps (squares). LAJ, Lajas Valley. Streams: LOC, Río Loco; N30−34, lower reach of Río Loco; YAU, Yauco; GUY, Guayanilla; MAC, Macaná; TAL, Tallaboa; MAT, Matilda; POR, Portugués; BUC, Bucaná; INA, Inabón; JAC, Jacaguas; DES, Descalabrado; COA, Coamo. Bedrock: LIM-par, Parguera Limestone; ER, El Rayo Formation; SG, Sabana Grande Formation; SERP, serpentinite; POB, two pyroxene olivine basalt; Y-bas; Yauco Formation basalt; Y-mud, Yauco Formation mudstone; GD, granodiorite; LG + MC, Yauco and Maricao Formations interbedded; LIM-jd, Juana Díaz Limestone; LIM-pon, Ponce Limestone; LG, Lago Garzas Formation; Y-congl, Yauco Formation conglomerate; MON, Monserrate Formation; LG + Y, Lago Garzas and Yauco Formations interbedded; COA, Coamo Formation; MV, Maravillas Formation; CARI, Cariblanco Formation.

2001). Basaltic and andesitic lava and volcanic breccia interfinger with volcaniclastic and calcareous sedimentary rocks and tuff and are intruded by felsic plutons (Jolly et al., 1998, 2007). Belts of serpentinite, which are metamorphosed ultramafic basement rocks of the upper mantle, occur in the southwest corner of the island, including in the Río Loco watershed (Lidiak et al., 2011). Wide and flat coastal plains consist of limestone interbedded with marine sedimentary deposits (Jolly et al., 1998). The southwest insular shelf is a carbonate platform up to 10 km wide and 18 m deep that contains emergent and submergent linear coral reefs on the shelf (Hernandez et al., 2009; Morelock et al., 1977) and deep reefs on the slope (García-Sais et al., 2008; Morelock et al., 1977). Winds are predominantly out of the east, are strongest during summer, and drive westward longshore currents (Cheriton et al., 2019; García--Sais et al., 2008; Warne et al., 2005). Waves approach the coast from the southwest, are more energetic in the summer and winter, and more quiescent from September through November (Cheriton et al., 2019; Hernandez et al., 2009; Sherman et al., 2013).

The island and insular shelf of Puerto Rico were impacted by two strong hurricanes during September 2017. Hurricane Irma passed approximately 100 km to the north of Puerto Rico on 6 September as a Category 5 storm, and on 20 September Hurricane Maria made landfall on the southeast coast as a Category 4 storm. It traveled northwest across the island over an 8-hr period and exited on the north-central coast (Fig. 1 inset). Heavy precipitation from Hurricanes Irma and Maria resulted in more than 40,000 landslides across Puerto Rico, mostly on steep hillslopes of the central mountainous region (Bessette-Kirton et al., 2019; Keellings and Hernández Ayala, 2019).

3. Methods

3.1. Sample collection

Sediment traps mounted on the seabed were deployed for 13 months starting in mid-May 2017 at 7 sites on the reef platform offshore and west of Guánica Bay (Fig. 1). Sediment traps consisted of paired 6.4-cm-diameter, 30-cm-long plastic tubes, which were attached side-by-side to a metal post driven into the reef substrate at approximately 10 m water depth and baffled with 1-cm-diameter mesh to prevent disturbance by organisms. Trap openings were 60 cm above the seabed. Trapped material was collected 6 times during the deployment, which lasted through mid-June 2018, at 6 to 11 week-long intervals. Traps S08 and S10 were upstream of Guánica Bay relative to the generally westward direction of alongshore flow, and traps S03–S07 and S11 were downstream. Waves and currents were measured at trap sites from June to December 2018; hydrodynamic processes are described elsewhere (Cheriton et al., 2019). Stream sediment ($n = 53$) and bedrock ($n = 19$) were collected from 13 drainages from Lajas Valley to Coamo River during 19–22 June 2017 (Fig. 1). Terrestrial sampling sites are shown in Fig. 1. Locations, descriptions, and geochemical data for all samples are available in Takesue (2019).

3.2. Bulk sediment properties

Sediment accumulation rates, sediment grain-size distributions, contents of organic, inorganic, and total carbon, and activities of the short-lived cosmogenic radionuclide beryllium-7 (^{7}Be, indicative of deposition during the previous 5 months) were measured in bulk trapped material. A sediment trap accumulation rate was calculated for each site and date from the average mass of air-dried material in the paired traps, the area of the trap opening, and the number of collection days per Storlazzi et al. (2011). Sediment accumulation rates are expressed in units of mg/cm^2/d and are referred to by the month and year of collection. Sediment grain-size distributions were determined on organic- and salt-free sediment using a combination of techniques. Particles with diameters >2 mm were separated by dry-sieving into quarter-phi intervals (size in mm = $2^{-\text{phi}}$) and weighed by size class. Sand and fine particles (0.063–2 mm and <0.063 mm, respectively) were separated by wet sieving and quantified by laser particle diffraction counting (Beckman Coulter Life Sciences). Grain size parameters were calculated according to Folk and Ward (1957). Total carbon (TC) and total inorganic carbon (TIC) of bulk sediment were determined coulometrically (UIC, Inc.). Total organic carbon (OC) was calculated as the difference between TC and TIC. The carbonate fraction of bulk trapped material was calculated as TIC multiplied by 8.333, the mass ratio of calcium carbonate to carbon.

Activities of ^{7}Be, determined on 10 ml of bulk sediment, are indicative of terrestrial inputs up to five months prior to sampling. Counts of ^{7}Be were acquired at 477.6 keV for 24–72 h in a low-background high-purity germanium (HPGe) well detector. The detector efficiency at 477.6 keV was interpolated from those at 351.9 keV (^{214}Pb) and 609.3 keV (^{214}Bi) using IAEA reference standard RGU-1 with similar geometries and counting times. Combined uncertainties include 1σ counting errors, detector efficiency, and background corrections.

3.3. Fine sediment and bedrock compositions

The fine fraction of sediment, or fines, consisting of particles with diameter <0.063 mm (silt and clay) was separated by dry sieving through stainless steel sieves. Bedrock was powdered to <0.075 mm-diameter particles. Approximately 2 g of fine material was sent to the USGS Analytical Chemistry Project, which subcontracted with AGAT Laboratories, a nationally accredited laboratory, for determinations of major oxides (bedrock only) and elemental contents, referred to here as compositions. Particles were decomposed by two methods for samples with sufficient fine-grained material: 1) a near-total four acid sediment digestion that quantified most major, minor, and trace elements, and 2) a total sediment digestion with a sodium peroxide fusion that quantified rare earth elements (REE) and elements such as chromium (Cr) and zirconium (Zr) that are hosted in refractory minerals (Morrison et al., 2009). Quantification was performed by inductively coupled plasma optical emission spectroscopy (ICP-OES) for major and some minor elements and inductively coupled plasma mass spectroscopy (ICP-MS) for some minor and all trace elements. Geologic reference materials, internal standards, and consistency standards were used for calibration, quality assurance, and quality control. Percent recoveries of all elements were within ±15% of certified values. Two sets of sample duplicates had average relative standard deviations (RSD) that were less than 7% for all target elements: aluminum (Al), calcium (Ca), magnesium (Mg), chromium (Cr), nickel (Ni), rubidium (Rb), scandium (Sc), vanadium (V), zirconium (Zr) and 14 rare earth elements, with the exception of cobalt (Co), which had an average RSD of 14%.

The total REE content (ΣREE) is the summed contents of the 14 REEs. The lanthanum to ytterbium ratio (La_N/Yb_N) is defined as the post-Archean Australian Shale [PAAS (Taylor and McLennan, 1985);]-normalized ratio of La to Yb. The europium (Eu) anomaly is defined as the ratio of the PAAS-normalized actual Eu content to the expected Eu content calculated as the geometric mean of PAAS-normalized contents of samarium (Sm) and gadolinium (Gd). Values of the Eu anomaly <1 are referred to as negative anomalies and >1 as positive anomalies.

StatPlusPro statistical software was used for Shapiro-Wilk normality tests, Spearman rank correlation, Pearson linear correlation, one-way analysis of variance (ANOVA), box plots, and descriptive statistics. Non-parametric statistics were used for non-normally distributed data. Box and whisker plots show the range between the first and third data quartiles (IQR), whiskers show maximum and minimum values. Outliers exceeding the IQR by a multiple up to 1.5 or 3.0 were excluded from calculations and are shown separately.

3.4. Geochemical sourcing with multivariate analysis

Certain elements are effective source indicators because they or their

ratios are transferred quantitatively into sediment from parent rocks during weathering, erosion, and transport, and are not significantly affected by diagenesis (McLennan et al., 1990). REE and their ratios are among the most reliable geochemical indicators in clastic sediment because different rock types can have distinct REE signatures, and once in the environment, most REEs exhibit similar behaviors (McLennan, 1989; Su et al., 2017). The major element aluminum (Al) behaves conservatively in clastic sediment (Fralick and Kronberg, 1997) as can certain trace elements such as chromium (Cr), cobalt (Co), nickel (Ni), rubidium (Rb), scandium (Sc), vanadium (V), and zirconium (Zr) (McLennan et al., 1990).

Principal component analysis (PCA), a multivariate technique, was used to distinguish the predominant patterns of geochemical variability, here referred to as geochemical signatures, in fine sediment from streams and in parent rocks on the southwest coast of Puerto Rico. Geochemical variables included: Al, Ca, Mg, Co, Cr, Ni, Rb, Sc, V, Zr, ΣREE, La_N/Yb_N, and the Eu anomaly. Seven representative types of local bedrock (2 basaltic, 2 andesitic, 1 felsic, 2 sedimentary) were included in the PCA of watershed geochemical signatures. PCA was performed on log transformed stream sediment and bedrock geochemical data in R Statistical Software using singular value decompositions of data matrices with standard normal distributions (R Core Team, 2018). Principal components (PC) with eigenvalues >1 were considered significant. Variable loadings and sample scores of opposite signs showed inverse geochemical relationships. Geochemical signatures determined by PCA in fine sediment collected in reef sediment traps were assumed to reflect watershed sources of material. The sample collected at S05 in August 2017 was excluded due to poor analytical performance. All geochemical variables except magnesium (Mg) were normally distributed in trapped fine sediment. Untransformed compositional data and log transformed Mg data were used in the sediment trap PCA. Hierarchical cluster analysis (HCA) based on Euclidean dissimilarities was used to explore spatial relationships among sites (R Core Team, 2018).

4. Results

4.1. Temporal and spatial variations of trapped sediment

Characteristics of trapped material provided temporal and spatial contexts for the May 2017 to June 2018 sediment trap study. There was a very large 80-fold range in sediment trap accumulation rates across the study area over 13 months, from 2 mg/cm^2/d at S08 in August 2017 to 167 mg/cm^2/d at S06 in November 2017 (Fig. 2a). Median sediment trap accumulation rates during the study exceeded 10 mg/cm^2/d, a health-effects threshold for certain corals (Rogers, 1990), except at traps S05 and S08 (Fig. 2a). Accumulation rates at S06 and S03 exceeded the threshold during every collection interval (Fig. 2a), whereas exceedances were slight at S07 and S10 (median = 11 mg/cm^2/d). Overall bulk carbonate fractions were 45% or higher and reached a maximum of 94% in traps S08 and S10 east of Guánica Bay in January 2018 (Fig. 2b). There was a moderate positive correlation between bulk carbonate fractions and accumulation rates among all sites and dates (Spearman $\rho = 0.49$, $p = 0.002$). There was a wide range in the fine fraction of sediment across the study area, from a winter minimum of 1% at S10 in

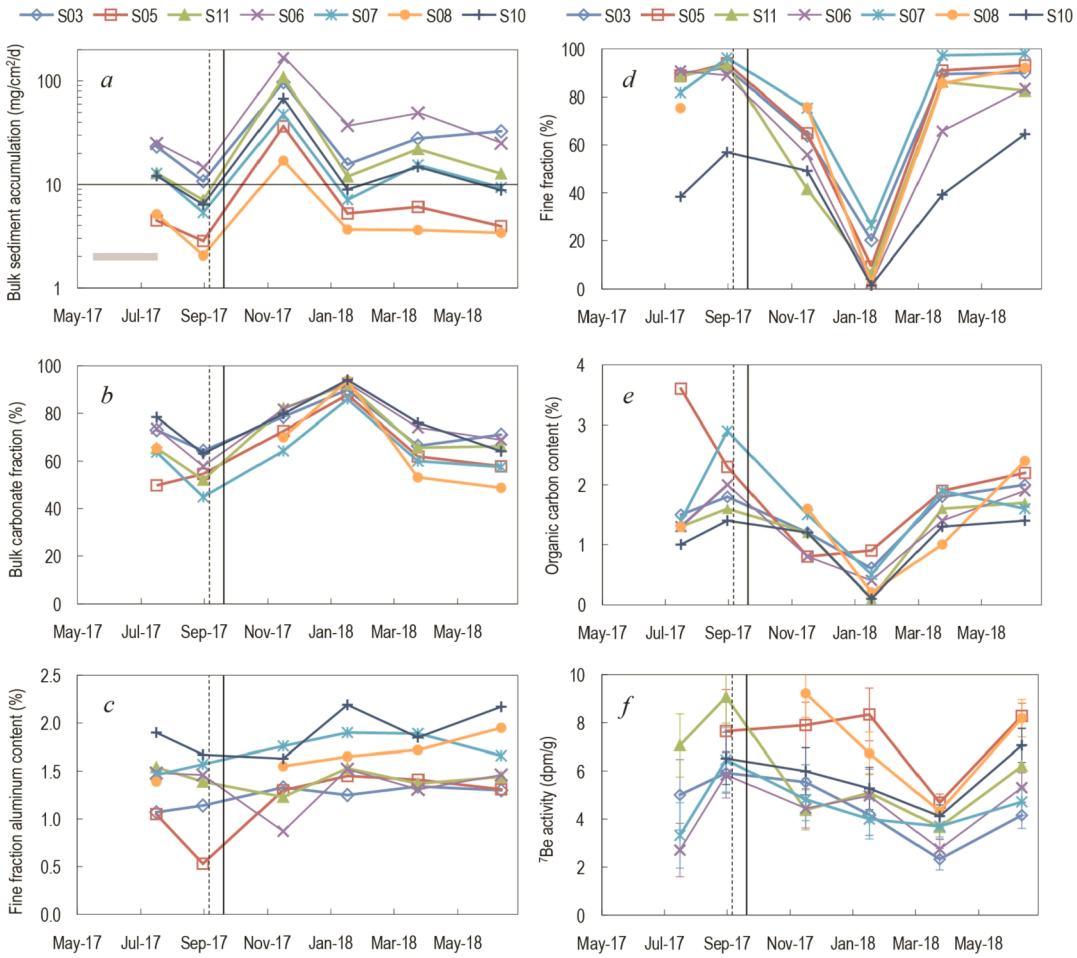

Fig. 2. Characteristics of sediment trap material through time. A) Bulk sediment trap accumulation rate plotted on a log scale; horizontal line shows 10 mg/cm^2/d, b) bulk carbonate content, c) fine fraction Al content, d) fine fraction, e) bulk organic carbon content, f) bulk ^{7}Be activity; error bars show combined uncertainties. Gray bar in 2a represents the first collection interval; symbols demarcate subsequent intervals. Dashed vertical line: Hurricane Irma, solid vertical line: Hurricane Maria.

January 2018 to a summer maximum of 98% at S07 in January 2018 (Fig. 2d). The fine fraction was inversely correlated with bulk carbonate among all sites and dates (Spearman $\rho = -0.83$, $p < 0.001$) but not with accumulation rates. Organic carbon contents varied over a narrow range, 0.1–3.6%, and were lowest in January 2018 (Fig. 2e). Activities of ^{7}Be (2.3–9.2 dpm/g) were generally lowest in March 2018 (Fig. 2f).

The seasonal variability in bulk sediment characteristics was greater than the spatial variability, evidenced by generally co-varying patterns through time among the 7 reef sites (Fig. 2). The median accumulation rate was highest (68 mg/cm^2/d) in material collected in November 2017 (Fig. 2a), and this material had intermediate bulk carbonate fractions, fine fractions, and organic carbon contents, indicative of mixed marine and terrestrial sources. In contrast, winter material collected in January 2018 had the highest median bulk carbonate fraction (92%; Fig. 2b) and the lowest median fine fraction (6%) and organic carbon content (0.4%), indicating a marine sediment source. The median accumulation rate and bulk carbonate fraction (6 mg/cm^2/d and 56%) were lowest in summer (July–August 2017) and were coupled with the highest median fine fraction and organic carbon content (93 and 1.9%) across the reef (Fig. 2a, b, d, e), indicative of terrigenous inputs.

The terrigenous content of the fine fraction of sediment was not measured directly; instead, the Al content of fine sediment was used as an indirect indicator because it is a major constituent of continental but not marine sediment (Fralick and Kronberg, 1997; Windom et al., 1989). Al contents ranged from 4.5 to 10.4% with a mean of 7.5 ± 1.2% (1σ, n = 50) in fine-grained stream sediment and from 0.9 to 2.2% with a mean of 1.5 ± 0.3% (1σ, n = 40) in sediment traps. By using the mean Al content of stream sediment (7.5%) and Ponce Limestone (0.2%) to represent terrestrial and marine carbonate end members, it was estimated that the fine fraction in sediment traps contained 9–27% terrigenous material. There were persistent spatial patterns in the delivery of terrigenous fine sediment to the reef (Fig. 2c): Al contents were higher at S07 (closest to the mouth of Guánica Bay) and S10 (east of the bay) than at S03 and S05 (west of the bay) ($p < 0.006$; Tukey-Kramer post-hoc tests). The same comparison for ΣREE, another terrestrial indicator, had similar results for the four western reef sites ($p < 0.006$, except for the comparison of S10 to S06, for which $p = 0.03$; Tukey-Kramer post-hoc tests). Thus, reef sites nearest to the mouth of Guánica Bay and up-current of Guánica Bay received the highest proportions of fine-grained terrigenous sediment among the reef sites. Al contents of fine trapped sediment increased over the study period by an average of 26 ± 9% (1σ) at all traps except S06 and S11 (Fig. 2c).

4.2. Geochemical signatures of watersheds from PCA and HCA

Four patterns of geochemical variability (4 significant PCs) described 84% of the variance in fine sediment and parent rocks collected from drainages on the southwest coast of Puerto Rico in June 2017. PC1 (41% of variance) was described by a covariance of Cr and Ni (negative loadings on PC1) inversely related to Ca content (positive loadings on PC1). A basalt containing pyroxene and olivine scored high on the Cr–Ni side of PC1, as did fine sediment from Río Loco (Fig. 3a). The high scores and tight clustering of Río Loco sediment indicated that Cr and Ni variability was characteristic of ultramafic rocks in this watershed. Calc-alkaline volcaniclastic and calcareous sedimentary rocks from the Coamo, Monserrate, and Yauco Formations scored high on the opposite side of PC1 (Fig. 3a), as did fine sediment from Ríos Bucaná, Descalabrado, and Jacaguas (Fig. 3a), which are underlain by those parent rocks.

PC2 (19% of variance) was described by inverse patterns of variance in Zr, an incompatible element, and covarying Sc and V, compatible elements associated with mafic rocks. Other incompatible element properties: ΣREE, Rb, and high La_N/Yb_N plotted near Zr on PC2, as did an andesite from the atypically-enriched El Rayo Formation (Jolly et al., 1998). Positive values of the Eu anomaly, typically associated with the mineral plagioclase, plotted with V and Sc on PC2, as did a basaltic andesite from the Largo Gazas Formation and fine sediment from Ríos Descalabrado, Coamo, and Matilda (Fig. 3a), located in the east near the city of Ponce.

PC3 (15% of variance) was indicative of felsic to intermediate volcanic rocks (Al) and calcareous sedimentary rocks (Ca) but was not a distinguishing signature among watersheds. Fine sediment from an upland site containing felsic granodiorite and dacite (GUY-3) scored high on the Al side of this component, and sediment from calcareous sedimentary rocks, such as from Río Bucaná (BUC-3) scored high on the Ca side of this component (Fig. 3b).

PC4 (9% of variance) was described by a covariation of the Eu anomaly with Rb, both associated with feldspar minerals. Basaltic and andesitic parent rocks scored high on PC4, as did fine sediment from a tributary of the Río Loco underlain by basalt (RLT-2) and from Río Descalabrado (DES-3) underlain by andesitic rocks (Fig. 3b). PC4 was not a distinguishing signature among watersheds.

Clustering of stream sediment geochemistry by longitudinal regions reflected west to east transitions of underlying rock types in southwest Puerto Rico from (ultra)mafic to felsic during the evolution of the magmatic island arc. Hierarchical cluster analysis showed that sediment

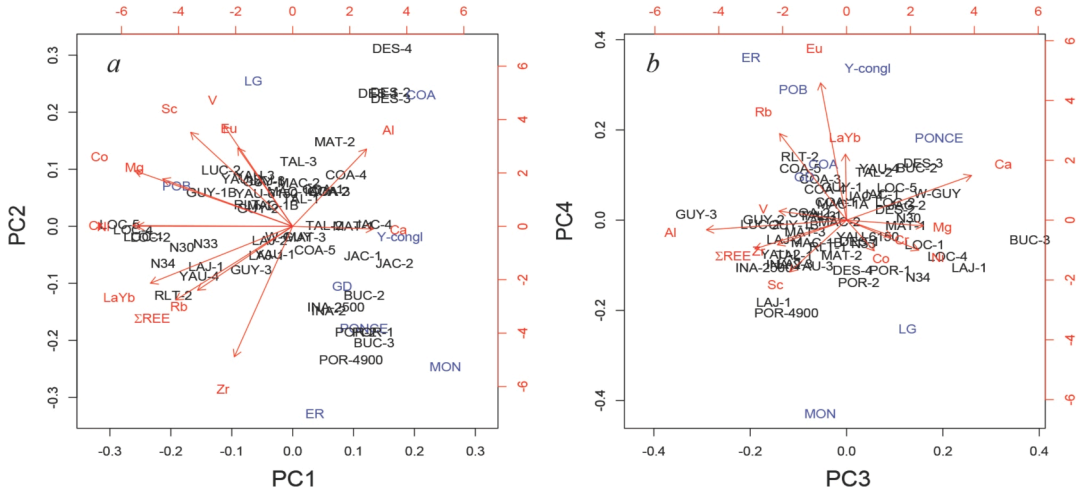

Fig. 3. Biplots showing principal component analysis (PCA) results for stream sediment and bedrock (blue) geochemistry. A) PC1 and PC2, b) PC3 and PC4. Arrows point to geochemical variable (red) loadings (right and top axes) and names show sample scores (left and bottom axes). ΣREE, total rare earth element content. Stream and bedrock locations are shown in Fig. 1 and described in Takesue (2019).

and parent rocks in Río Loco watershed formed a cluster that was geochemically distinct from all other drainages (Fig. 4). The remaining sites fell into two geographically distinct geochemical clusters. Streams discharging into Guayanilla Bay (Yauco, Guayanilla, Macaná) and to the adjoining coastal region at Tallaboa clustered together. The geographic outliers in this cluster were sediment from a Río Loco tributary (RLT-2) and sediment from Río Matilda (MAT-3). The upper reaches of RLT-2 are underlain by the Yauco Formation, explaining its inclusion in a more mafic cluster relative to its geographic position and indicating that sediment was sourced from higher elevations. Similarly, the upper reaches of Río Matilda are underlain by basaltic rocks of the Lago Garzas Formation, explaining its inclusion in a more mafic cluster. Streams between Ponce and Coamo formed another geochemical cluster that also included sediment from Río Guayanilla and its mouth (GUY-3, W-GUY), which were influenced by material from a felsic pluton of granodiorite in the upper watershed.

4.3. Geochemical signatures in sediment traps from PCA

Four significant PCs described 90% of the compositional variance in fine sediment collected in sediment traps from May 2017 to June 2018. The first PC had a spatial component that was also temporally persistent, the second PC had only a spatial component, and the third and fourth PCs had only temporal components.

PC1 (51% of variance) was characterized by high positive covariations of Al, V, and Sc (Fig. 5a), the geochemical signature of watersheds east of Guánica Bay underlain by andesitic volcanic rocks. Positive scores on PC1 were highest in traps upstream of Guánica Bay (S08, S10) and outside of the bay mouth (S07) (Fig. 6a and b).

PC1 was the only component with a consistent spatial pattern throughout the study period: site S10 scored highest on PC1 and there was a general westward decrease in scores downstream (Fig. 6a and b). La_N/Yb_N ratios characterized the inverse pattern of variability on PC1 (Fig. 6a), such that ratios were high in fine sediment that had low Al, V, and Sc contents. Fine-grained stream sediment from the local Río Loco drainage and its tributary (RLT-2) had some of the highest La_N/Yb_N ratios, and likely contributed to high negative scores on PC1 in traps west of the mouth of Guánica Bay.

PC2 (19% of variance) was characterized by a positive covariance of Cr and Ni (Fig. 5a), the geochemical signature of ultramafic Río Loco sediment. Sites down-current of Guánica Bay (S03, S06, S07, S11) had higher median scores on PC2 than up-current sites (S08, S10) except for S05 (Fig. 6d). More specifically, trapped sediment at sites S06 or S07, in closest proximity to the mouth of Guánica Bay, scored highest on PC2 for all six collection intervals (Fig. 6c and d). High negative loadings on PC2 were characterized by elevated Mg with low Cr and Ni, and occurred at sites S05, S08, and S10 (Fig. 6c and d). Volcaniclastic sedimentary rocks of the Monserrate and Coamo Formations, which underlie watersheds east of Ponce, had these characteristics.

PC3 (11% of variance) was characterized by variations of the Eu anomaly and Ca that were inversely related to variations of Mg and Ni (Fig. 5b). Six of seven sediment traps collected in November 2017 after Hurricanes Irma and Maria scored high on PC3 (Figs. 5b and 6e). There were no significant differences in Al and Cr contents compared to the preceding month (one-way ANOVA), but Mg was 27% lower and Ni was 45% lower (one-way ANOVA, $p < 0.001$ and $p = 0.03$, Tukey post-hoc test). This decoupling of Cr and Ni was inconsistent with a local Río Loco signature in November 2017 traps. Only S07, offshore of the mouth of Guánica Bay, had covarying Cr, Ni, and Al, indicative of local sediment in the months following Hurricanes Irma and Maria.

PC4 (8% of variance) was characterized by opposing patterns of variability of the Eu anomaly and La_N/Yb_N ratios (Fig. 5b), the geochemical signatures of mafic and felsic volcanic rocks. There was a moderate inverse correlation between Eu anomalies and La_N/Yb_N ratios in trapped sediment with negative scores on PC4 (Pearson $r = -0.48$, $p = 0.06$), characteristics of the Ríos Portugués and Descalabrado drainages east of Ponce. This geochemical signature only appeared offshore and west of Guánica Bay in March and June 2018 (Fig. 6g).

5. Discussion

An island-wide assessment concluded that runoff impacts to coral reef ecosystems of Puerto Rico were determined by coastal transport of sediment and contaminants by wind-driven currents and waves (Larsen and Webb, 2009; Warne et al., 2005). Local studies at southwest Puerto Rico reefs found that overall sediment trap accumulation rates were related to wave exposure, and high accumulation rates were caused by storm-wave-driven bottom sediment resuspension rather than inputs of new terrigenous material (Hernandez et al., 2009; Sherman et al., 2013). During the current study, the largest waves occurred at a site on a coastal promontory (S06) and the smallest ones at a site in the lee of the promontory (S03), corresponding to bottom sediment resuspension approximately 75 and 25% of the year, respectively, for carbonate sand $\leq$0.500 mm and terrigenous silt $\leq$0.004 mm (Cheriton et al., 2019). Despite these contrasting physical conditions, S03 and S06 had the highest median sediment trap accumulation rates, indicating that both hydrodynamic regimes were conducive to accumulation on the coral reefs. The ecological implications were different for the two sites, however. Compared to the energetic site, material that accumulated at the protected site was finer-grained and had more organic matter, both characteristics that can impart greater physiological stress on corals (Fabricius, 2005; Weber et al., 2006, 2012). High sediment trap accumulation rates at the protected site (S03), where wave energy was lower, can be explained by settling of particles advected in suspension by

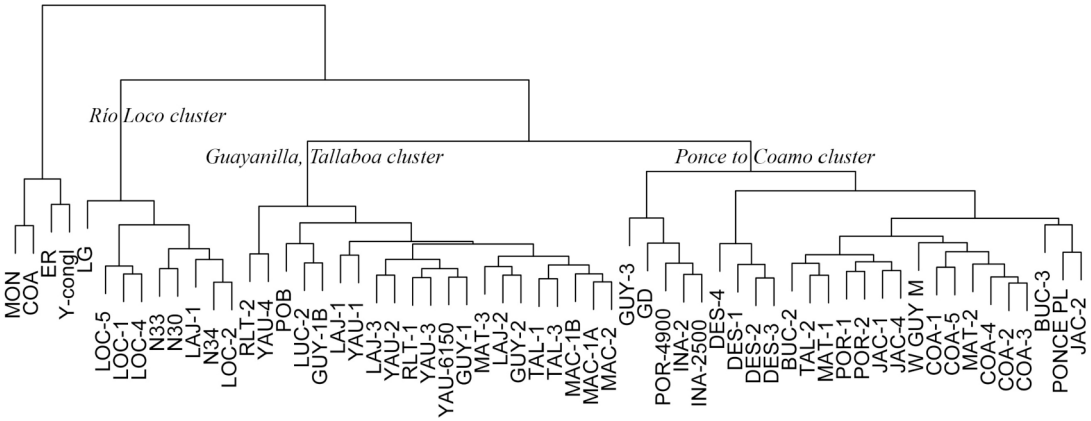

Fig. 4. Hierarchical cluster diagram showing groupings of geochemically similar stream sediments (n = 53) and parent rocks (n = 7) that generally correspond to the geography of southwest Puerto Rico. Stream and bedrock locations are shown in Fig. 1 and described in Takesue (2019).

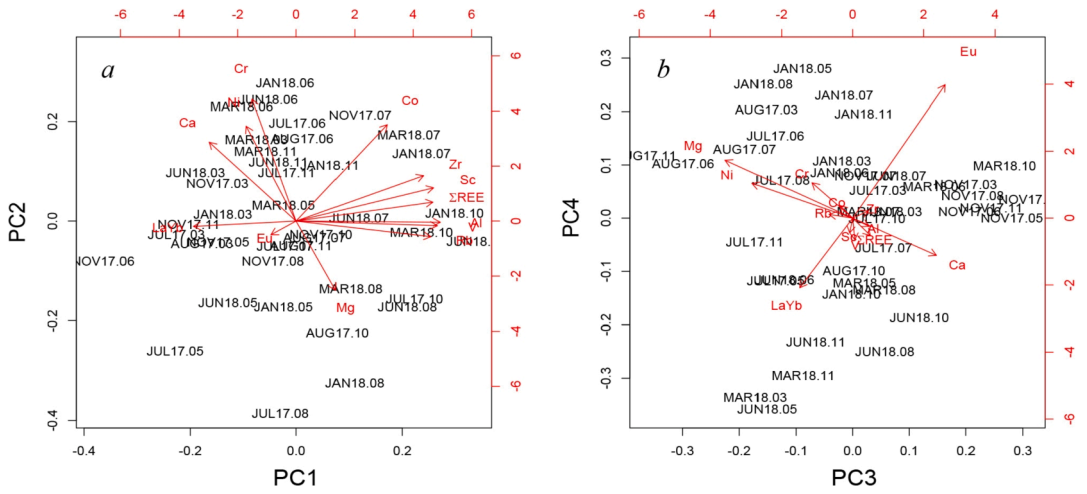

Fig. 5. Biplots showing principal component analysis (PCA) results for fine-grained trapped sediment. A) PC1 and PC2, b) PC3 and PC4. Arrows point to geochemical variable (red) loadings (right and top axes) and trap names show sample scores (left and bottom axes). Samples are labeled with the month and two-digit year of collection followed by the sediment trap number, e.g., JUL17.08 indicates trap 08 collected in July 2017. Sediment trap locations are shown in Fig. 1.

alongshore currents. Westward advection of material from Guánica Bay was inferred by Otero and Carbery (2005) to explain higher turbidity at a protected reef compared to other mid-shelf reefs. Geochemical signatures from this study confirm that S03 was strongly influenced by advected runoff from Río Loco/Guánica Bay (high negative scores on PC1). Both the nature and source of sediment settling at S03 posed a greater health risk to corals because Guánica Bay sediment contains elevated levels of pesticides, polychlorinated biphenyls (PCBs), and polycyclic aromatic hydrocarbons (PAHs) (Kumar et al., 2016; Pait et al., 2008b; Whitall et al., 2014). In contrast, no contaminants were found at levels of concern in coral tissue collected in the energetic month of June at reef sites corresponding to wave-exposed sites in this study (Whitall et al., 2014), demonstrating the importance of physical processes in the health of reef ecosystems.

Advected terrigenous sediment originating in watersheds 20 km or more upcoast was a major component of fine-grained material trapped at two sites east of Guánica Bay– Aurora Cay (S10) and a nearby submerged reef (S08), and at a site outside of the bay mouth (S07). The importance of distally advected material decreased west of Guánica Bay. Persistent inputs of distally advected sediment to this region of the southwest Puerto Rico coast throughout the study period indicates that terrigenous sediment runoff to the coastal ocean was ongoing through June 2018. The Al content of the fine fraction in sediment traps did not decrease in the months following the rainy season, as would be the case if deposits of terrigenous material on the seabed were progressively winnowed. Several studies suggest that mass wasting and sediment runoff to the coast persisted long after the passage of Hurricane Maria, including ground-based assessments (Bessette-Kirton et al., 2019); a land surface model that predicted enhanced erosion and runoff due to defoliation, high soil moisture, and ongoing rainfall through November 2017 (Miller et al., 2018); and remote sensing observations of elevated nearshore turbidity through February 2018 (Miller et al., 2018) and chlorophyll-*a* through December 2017 (Hernandez et al., 2020). Mass wasting events can also affect sediment delivery to the coast for years or decades if sediment is stored in lowlands or river channels and mobilized by subsequent storms (Larsen and Webb, 2009). Activities of ^{7}Be shifted to lower values at all 7 reef sites in material collected from mid-January to mid-March 2018 when other properties such as lower bulk carbonate fraction, higher fine fraction, and higher organic carbon content indicated that there was an increase in the terrigenous fraction in trapped material. In combination, these properties could reflect delayed delivery of surface sediment that was initially mobilized, stored in a basin over a period of months, then remobilized and transported to the coastal ocean.

The west-to-east geological and geochemical gradient across southwest Puerto Rico watersheds enabled distal sediment inputs to be distinguished from local ones based on geochemical signatures in runoff to the southwest coast. The small yet significant component of advected sediment (8% of variance) ascribed to Ríos Portugués and Descalabrado in mid-March and mid-June 2018 demonstrates the discerning power of PCA geochemical signatures in southwest Puerto Rico. This tool can be applied in other areas with distinct source rocks to assess sediment delivery patterns associated with changes in land use, hydroclimatology, watershed restoration, and extreme events such as hurricanes.

5.1. *Impacts of Hurricanes Irma and Maria on reef sediment accumulation and sourcing*

Large storms, including hurricanes, cause dramatic changes in coastal sedimentary environments and are credited with removal, or flushing, of sediment deposits from areas typically sheltered from waves and currents (Cheriton et al., 2019; DeMartini et al., 2013; Draut et al., 2009; Hernandez et al., 2009; Lugo-Fernández et al., 1994; Sherman et al., 2013). Though intense, storm-driven flushing events are short-lived, ending when the storm propagates out of the area (Cheriton et al., 2019; Hernandez et al., 2009; Sherman et al., 2013). The current sediment trap time series included an interval from September to mid-November 2017 in which Hurricane Irma, Hurricane Maria, and a large October storm caused bottom sediment resuspension (Cheriton et al., 2019) and high sediment trap accumulation rates on the southwest Puerto Rico shelf. It was not possible, however, to uniquely attribute the altered characteristics of sediment collected during this interval to the hurricanes, because a previous sediment trap study measured similar changes after a large non-hurricane October storm (Sherman et al., 2013). In addition, material trapped during the 2.5-month-long collection interval September to mid-November 2017 was an integration of storm deposits and post-storm runoff during a season with otherwise calm oceanographic conditions that favored the settling of fine-grained material (Cheriton et al., 2019). Rather, the value of the current 13-month-long sediment trap study was from insights about longer-term exports of sediment from coastal watersheds likely caused by hurricane-related alterations of landscapes and runoff patterns. These larger-scale alterations could have lasting, if different, impacts to nearshore ecosystems compared to those resulting directly from storm forcing, especially if they introduce contaminants to coastal ecosystems from urbanized watersheds and persist into ecologically sensitive spawning and recruitment windows in summer and fall (de Graaf et al., 1999; van Veghel, 1994; van Woesik et al., 2006).

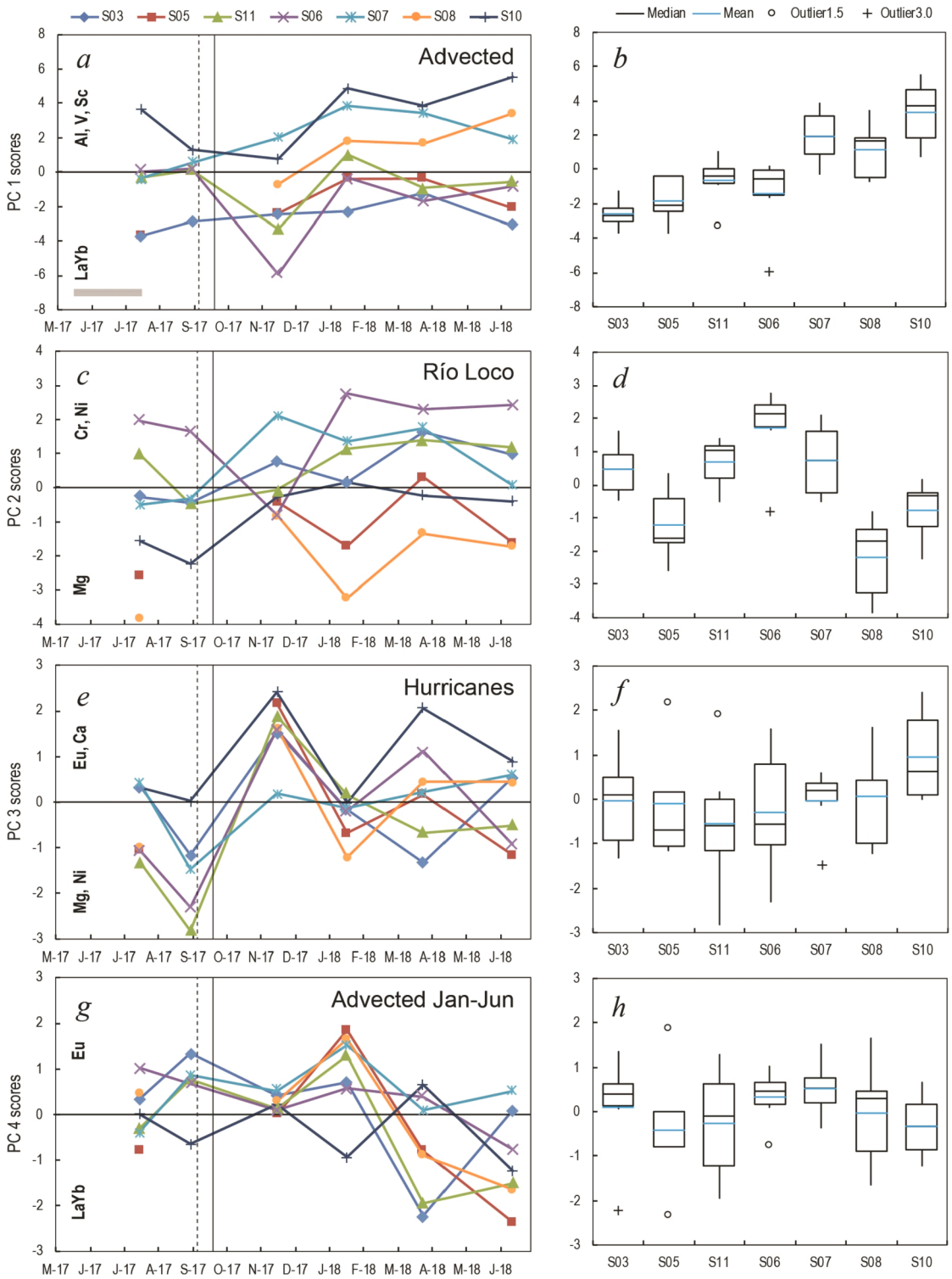

Fig. 6. Principal component (PC) scores in the sediment trap fine fraction by date (left) and site (right). a, b) PC1; c, d) PC2; e, f) PC3; g, h) PC4. The first collection interval is shown by the gray bar; symbols demarcate subsequent intervals. Dashed vertical line: Hurricane Irma, solid vertical line: Hurricane Maria.

5.2. Runoff sourcing and hydrodynamics

Reef sites offshore and downcoast to the west of Guánica Bay were not equally affected by fine sediment settling, nor by the same sources of runoff, and these findings have implications for nearshore ecosystem protection and remediation. The area outside of the mouth of Guánica Bay appeared to be a region where the direction of flow fluctuated. The area primarily received fine sediment advected westward from distal watersheds upcoast, likely due to its orientation facing predominant wind, wave, and current directions. Southward flow out of Guánica Bay carrying fine sediment from the local Río Loco watershed was of secondary importance. The exception to this pattern occurred during the 2.5 month-long collection interval from September to mid-November 2017 that included Hurricanes Irma and Maria, when the site offshore of the bay mouth was the only one more strongly dominated by local rather than distal runoff. Given the site's proximity to a runoff source

and position along the outflow path, it seems likely that reef communities in this area were influenced by the local watershed intermittently during storms, and by distal watersheds the rest of the year. Storm runoff can have a lasting effect on organisms, because corals offshore of the mouth of Guánica Bay were found in June 2009 to have elevated tissue contents of PAHs and PCBs of bay origin (Whitall et al., 2014) following a wet rainy season and dry spring (USGS, 2016). It is also possible that large industrial and urban centers in watersheds upcoast to the east of Guánica were sources of sediment-bound contaminants to downstream corals and other biota. For example, power plants like the one in Guayanilla are known sources of PCBs and PAHs; oil refining, storage, and transport facilities such as the one in Peñuelas are known sources of PAHs, and runoff from urban centers like Ponce can contain PCBs and PAHs (e.g., Erickson and Kaley, 2011; Hoffman et al., 1984; Wolska et al., 2012). Insights from sediment trap time series about the timing and persistence of potentially contaminant-laden sediment inputs can inform how, where, and when to implement measures to reduce the export of sediment and sediment-bound contaminants to coastal ecosystems.

The reef site at Terramoto Cay (S05) was unique because it was in an exposed position on the mid-shelf but had the second-lowest median sediment trap accumulation rates and was not strongly influenced by runoff from the Río Loco/Guánica Bay watershed, evidenced by an inverse pattern of variance relative to the Río Loco geochemical signature. Wave energy was similar at Terramoto Cay and outside of the mouth of Guánica Bay, whereas many of the bulk sedimentary characteristics at Terramoto Cay were similar to those at a more protected submerged reef (S08) upstream of Guánica Bay. One possible explanation for the mixed sedimentary properties at Terramoto Cay is that it was the most distant site from shore situated 1.6 km west of a promontory and 2.3 km south of the shoreline. If distance from shore was the determining factor in the type of sediment reaching Terramoto Cay, this would suggest that runoff from Guánica Bay was advected westward in a narrow band close to shore, whereas fine sediment advected from distal watersheds upcoast to the east was transported westward farther offshore over the mid-shelf. A more detailed description of circulation patterns downstream of Guánica Bay would aid in understanding suspended sediment and sediment-bound contaminant transport to reef sites and could inform site selection for ecological studies aiming to quantify sediment and contaminant impacts of Río Loco/Guánica Bay outflows. García-Sais et al. (2008) described distance-dependant flow patterns in La Parguera Nature Reserve, 11 km west of Guánica Bay, where local runoff was entrained close to shore and reefs more than 2 km from shore were influenced by upstream rather than local runoff sources.

5.3. *Implications for coastal ecosystem protection and restoration*

Suspended sediment, nutrient, and other contaminant fluxes from human disturbances in catchments to coastal ecosystems are increasing in many locations (Bartley et al., 2014; Meybeck and Vorosmarty, 2005), as are intensities of natural disturbances such as storms that trigger land-to-sea material exports (Du et al., 2019; Swain et al., 2020; Trenberth, 2005). Runoff management and coastal ecosystem protection require understanding about sources and transport processes, information that geochemical signatures in sediment can provide (Bainbridge et al., 2016; Douglas et al., 2006; Yang and Youn, 2007). Geochemical signatures in the fine fraction of trapped sediment provided many insights about the sources, timing, and transport of land-derived runoff to coral reef ecosystems in southwest Puerto Rico that have implications for runoff management and watershed restoration. One important new finding was that a large component of fine sediment trapped on reefs was advected from distal watersheds. Thus, a complete understanding of ecosystem risk at these sites from sediment and sediment-bound contaminants will require characterization of distal sources, and the successful reduction of contaminant loads to downstream ecosystems could require mitigation measures over broad spatial scales and involve multiple jurisdictions and decision-making bodies (Alvarez-Romero et al., 2015; Pittman and Armitage, 2016). Second, geochemical signatures confirmed that the local Río Loco/Guánica Bay watershed was the source of fine sediment and sediment-bound contaminants found by previous studies at reef sites down-current to the west (García-Sais et al., 2008; Pait et al., 2008b; Sherman et al., 2013; Whitall et al., 2014) and additionally that the flow of local runoff was confined close to shore. As a result, assessment and mitigation of ecological impacts from local runoff should be explored on the inner shelf, rather than at mid-shelf. Third, the months-long persistence of sediment runoff from distal watersheds showed the lasting influence of hurricane-induced landscape-scale change on sediment delivery to the coastal ocean and its potential long-term impacts on downstream ecosystems. Such large perturbations in sediment supply could attenuate over months or years before returning to pre-storm conditions, and consideration of both system-response timeframes would improve the effectiveness of sediment management strategies in coastal catchments (e.g., Clark and Wilcock, 2000; James, 1999; Thrush et al., 2004). Finally, geochemical differences in upland and lowland tributary sediment in Río Loco and Río Matilda allowed attribution of active runoff to upper watersheds, signaling that mitigation initiatives at higher elevations in these basins would have a greater impact on runoff reduction than ones on the urbanized coastal plain. Sediment geochemical sourcing, particularly when combined with nearshore sediment traps, provides needed understanding for natural resource managers aiming to mitigate harmful effects of runoff from developing coastal watersheds (Barragan and de Andres, 2015; Mee, 2012; Small and Nicholls, 2003) to nearshore ecosystems.

6. Conclusions

Geochemical signatures in fine sediment collected during a 13 month-long sediment trap study, co-located with wave and current measurements, and integrated with watershed sediment characterization provided new understanding about the importance of local versus distal sources of land-derived sediment runoff to coral reef ecosystems, long-term impacts of Hurricane Maria on terrigenous sediment delivery to the coastal ocean, and nearshore transport patterns at the southwest coast of Puerto Rico. Geochemical signatures defined by multivariate principal component analysis showed that fine sediment was advected westward from upcoast watersheds 20 km or more distant and represented the largest component of geochemical variance in suspended sediment east and offshore of Guánica Bay. Runoff from the local Río Loco watershed was advected westward in a narrow band along the coast where its ecological impacts would be the greatest, and only appeared at mid-shelf reef sites following storms when winds were directed offshore. Hurricane Maria, which crossed the island on September 20, 2017 as a Category 4 storm, caused landscape-scale changes in vegetation cover, soil moisture, mass wasting, and nearshore turbidity, and effects of these changes were reflected in persistent runoff and westward advection of fine sediment to reef traps offshore and downstream of Guánica Bay at least through June 2018 when the study ended. Sediment geochemical sourcing combined with nearshore sediment traps are a powerful tool that can increase understanding about land-derived runoff sources, timing, and nearshore transport and guide watershed management and ecosystem restoration strategies.

Submission declaration

All authors agree to the submission.

CRediT author statement

Renee Takesue: Conceptualization, Methodology, Investigation, Formal analysis, Writing - Original Draft, Data Curation; Clark Sherman: Conceptualization, Resources, Project administration, Supervision,

Funding acquisition; Natalia Ramirez: Investigation; Aaron Reyes: Investigation, Writing - Review & Editing; Olivia Cheriton: Formal analysis; Roberto Viqueira Ríos: Conceptualization; Curt Storlazzi: Conceptualization, Resources, Writing - Review & Editing, Project administration, Supervision, Funding acquisition.

Declaration of competing interest

The authors declare that they have no known competing financial interests or personal relationships that could have appeared to influence the work reported in this paper.

Acknowledgements

The authors thank the Magueyes Island Marine Laboratories of the University of Puerto Rico at Mayagüez for lab and field support; Dave Whitall (NOAA) for assistance with sample collection; Angela Tan (USGS) and Leticia Hallas (USGS) for assistance processing samples; Carsten Braun (WSU) for assistance with ArcGIS; and a USGS reviewer and two anonymous reviewers for suggestions that improved the manuscript. This work was funded by the U.S. Geological Survey's Coastal and Marine Hazards and Resources Program, and by the National Oceanographic and Atmospheric Administration's Coral Reef Conservation Program (Grant NA15NOS4820073). Any use of trade, firm, or product names is for descriptive purposes only and does not imply endorsement by the U.S. Government. Although this information product, for the most part, is in the public domain, it also may contain copyrighted materials as noted in the text. Permission to reproduce copyrighted items must be secured from the copyright owner.

References

Acevedo, R., Morelock, J., Olivieri, R.A., 1989. Modification of coral reef zonation by terrigenous sediment stress. Palaios 4, 92–100. https://doi.org/10.2307/3514736.

Alvarez-Romero, J.G., Adams, V.M., Pressey, R.L., Douglas, M., Dale, A.P., Auge, A.A., Ball, D., Childs, J., Digby, M., Dobbs, R., Gobius, N., Hinchley, D., Lancaster, I., Maughan, M., Perdrisat, I., 2015. Integrated cross-realm planning: a decision-makers' perspective. Biol. Conserv. 191, 799–808. https://doi.org/10.1016/j.biocon.2015.07.003.

Anderson, C.H., Murray, R.W., Dunlea, A.G., Giosan, L., Kinsley, C.W., McGee, D., Tada, R., 2018. Climatically driven changes in the supply of terrigenous sediment to the East China Sea. G-cubed 19, 2463–2477. https://doi.org/10.1029/2017GC007339.

Araújo, M.F., Jouanneau, J.-M., Valério, P., Barbosa, T., Gouveia, A., Weber, O., Oliveira, A., Rodrigues, A., Dias, J.M.A., 2002. Geochemical tracers of northern Portuguese estuarine sediments on the shelf. Prog. Oceanogr. 52, 277–297. https://doi.org/10.1016/j.csr.2004.02.010.

Bainbridge, Z., Lewis, S., Smithers, S., Wilkinson, S., Douglas, G., Hillier, S., Brodie, J., 2016. Clay mineral source tracing and characterisation of Burdekin River (NE Australia) and flood plume fine sediment. J. Soils Sediments 16, 687–706. https://doi.org/10.1007/s11368-015-1282-4.

Barragan, J.M., de Andres, M., 2015. Analysis and trends of the world's coastal cities and agglomeration. Ocean Coast Manag. 114, 11–20. https://doi.org/10.1016/j.ocecoaman.2015.06.004.

Bartley, R., Bainbridge, Z.T., Lewis, S.E., Kroon, F.J., Wilkinson, S.N., Brodie, J.E., Silburn, D.M., 2014. Relating sediment impacts on coral reefs to watershed sources, processes, and management: a review. Sci. Total Environ. 468–469, 1138–1153. https://doi.org/10.1016/j.scitotenv.2013.09.030.

Bessette-Kirton, E.K., Cerovski-Darriau, C., Schultz, W.H., Coe, J.A., Kean, J.W., Godt, J. W., Thomas, M.A., Hughes, K.S., 2019. Landslides triggered by Hurricane Maria: assessment of an extreme event in Puerto Rico. GSA Today (Geol. Soc. Am.) 29, 4–10. https://doi.org/10.1130/GSATG383A.1.

Brodie, J., Pearson, R.G., 2016. Ecosystem health of the Great Barrier Reef: time for effective management action based on evidence. Estuar. Coast Shelf Sci. 183, 438–451. https://doi.org/10.1016/j.ecss.2016.05.008.

Carriger, J.F., Fisher, W.S., Stockton, T.B., Sturm, P.E., 2013. Advancing the Guánica Bay (Puerto Rico) watershed management plan. Coast. Manag. 41, 19–38. https://doi.org/10.1080/08920753.2012.747814.

Cheriton, O.M., Storlazzi, C.D., Rosenberger, K.J., Sherman, C., 2019. Controls on sediment transport over coral reefs off southwest Puerto Rico: seasonal patterns and Hurricane Maria. In: Wang, P., Rosati, J.D., Vallee, M. (Eds.), International Conference on Coastal Sediments 2019, Proceedings of the 9th International Conference, pp. 903–915. Tampa/St. Petersburg, Florida, USA.

Clark, J.J., Wilcock, P.R., 2000. Effects of land-use change on channel morphology in northeastern Puerto Rico. Geol. Soc. Am. Bull. 112, 1763–1777. https://doi.org/10.1130/0016-7606(2000)112<1763:EOLUCO>2.0.CO;2.

Costanza, R., de Groot, R., Sutton, P., van der Ploeg, S., Anderson, S.J., Kubiszewski, I., Farber, S., Turner, R.K., 2014. Changes in the global value of ecosystem services. Global Environ. Change 26, 152–158. https://doi.org/10.1016/j.gloenvcha.2014.04.002.

Day, J.W., Agboola, J., Chen, Z., D'Elia, C., Forbes, D.L., Giosan, L., Kemp, P., Kuenzer, C., Lane, R.R., Ramachandran, R., Syvitski, J., Yanez-Arancibia, A., 2016. Approaches to defining deltaic sustainability in the 21st century. Estuar. Coast Shelf Sci. 183, 275–291. https://doi.org/10.1016/j.ecss.2016.06.018.

de Graaf, M., Geertjes, G.J., Vudeker, J.J., 1999. Observations on spawning of scleractinian corals and other invertebrates on the reefs of Bonaire (Netherlands Antilles, Caribbean). Bull. Mar. Sci. 64, 189–194.

DeMartini, E., Jokiel, P., Beets, J., Stender, Y., Storlazzi, C., Minton, D., Conklin, E., 2013. Terrigenous sediment impact on coral recruitment and growth affects the use of coral habitat by recruit parrotfishes (*F. scaridae*). J. Coast Conserv. 17, 417–429. https://doi.org/10.1007/s11852-013-0247-2.

Douglas, G.B., Ford, P.W., Palmer, M., Noble, R.M., Packett, R., 2006. Fitzroy River, Queensland, Australia. II. Identification of sources of estuary bottom sediments. Environ. Chem. 3, 377–385. https://doi.org/10.1071/EN06010.

Draut, A.E., Bothner, M.H., Field, M.E., Reynolds, R.L., Cochran, S.A., Logan, J.B., Storlazzi, C.D., Berg, C.J., 2009. Supply and dispersal of flood sediment from a steep, tropical watershed: hanalei Bay, Kaua'i, Hawai'i, USA. Geol. Soc. Am. Bull. 121, 574–585. https://doi.org/10.1130/B26367.1.

Du, H., Alexander, L.V., Donat, M.G., Lippmann, T., Srivastava, A., Salinger, J., Kruger, A., Choi, G., He, H.S., Fujibe, F., Rusticucci, M., Nandintsetseg, B., Manzanas, R., Rehman, S., Abbas, F., Zhai, P., Yabi, I., Stambaugh, M.C., Wang, S., Batbold, A., Teles de Oliveira, P., Adrees, M., Hou, W., Zong, S., Moises Santos e Silva, C., Lucio, P.S., Wu, Z., 2019. Precipitation from persistent extremes is increasing in most regions and globally. Geophys. Res. Lett. 46, 6041–6049. https://doi.org/10.1029/2019GL081898.

Duarte, C.M., 2009. Return to Neverland: shifting baselines affect eutrophication restoration targets. Estuar. Coast 32, 29–36. https://doi.org/10.1007/s12237-008-9111-2.

Erickson, M.D., Kaley, R.G., 2011. Applications of polychlorinated biphenyls. Environ. Sci. Pollut. Res. 18, 135–151. https://doi.org/10.1007/s11356-010-0392-1.

Fabricius, K.E., 2005. Effects of terrestrial runoff on the ecology of corals and coral reefs: review and synthesis. Mar. Pollut. Bull. 50, 125–146. https://doi.org/10.1016/j.marpolbul.2004.11.028.

Folk, R.L., Ward, W.C., 1957. Brazos River bar [Texas]; a study in the significance of grain size parameters. J. Sediment. Res. 27, 3–26. https://doi.org/10.1306/74D70646-2B21-11D7-8648000102C1865D.

Fralick, P.W., Kronberg, B.I., 1997. Geochemical discrimination of clastic sedimentary rock sources. Sediment. Geol. 113, 111–124. https://doi.org/10.1016/S0037-0738(97)00049-3.

García-Sais, J., Appeldoorn, R., Battista, T., Bauer, L.J., Bruckner, A., Caldow, C., Carrubba, L., Corredor, J., Diaz, E., Lilyestrom, C., García-Moliner, G., Hernández-Delgado, E., Menza, C., Morell, J., Pait, A., Sabater, J., Weil, E., Williams, E., Williams, S., 2008. The state of coral reef ecosystems of Puerto Rico. In: Waddell, J. E., Clarke, A.M. (Eds.), The State of Coral Reef Ecosystems of the United States and Pacific Freely Associated States: 2008, 73. NOAA Technical Memorandum NOS NCCOS, Silver Springs, MD, pp. 75–116.

Gellis, A.C., Mukundan, R., 2013. Watershed sediment source identification: tools, approaches, and case studies. J. Soils Sediments 13, 1655–1657. https://doi.org/10.1007/s11368-013-0778-z.

Hernandez, R., Sherman, C., Weil, E., Yoshioka, P., 2009. Spatial and temporal patterns in reef sediment accumulation and composition, southwestern insular shelf of Puerto Rico. Caribb. J. Sci. 45, 138–150.

Hernandez, W.J., Ortiz-Rosa, S., Armstrong, R.A., Geiger, E.F., Eakin, C.M., Warner, R.A., 2020. Quantifying the effects of Hurricanes Irma and Maria on coastal water quality in Puerto Rico using moderate resolution satellite sensors. Rem. Sens. 12, 964. https://doi.org/10.3390/rs12060964.

Hoffman, E.J., Mills, G.L., Latimer, J.S., Quinn, J.G., 1984. Urban runoff as a source of polycyclic aromatic hydrocarbons to coastal waters. Environ. Sci. Technol. 18, 580–587. https://doi.org/10.1021/es00126a003.

James, L.A., 1999. Time and persistence of alluvium: river engineering, fluvial geomorphology, and mining sediment in California. Geomorphology 31, 265–290. https://doi.org/10.1016/S0169-555X(99)00084-7.

Jolly, W.T., Lidiak, E.G., Dickin, A.P., Wu, T.W., 2001. Secular geochemistry of central Puerto Rican island arc lavas: constraints on Mesozoic tectonism in the eastern Greater Antilles. J. Petrol. 42, 2197–2214. https://doi.org/10.1093/petrology/42.12.2197.

Jolly, W.T., Lidiak, E.G., Schellekens, J.H., Santos, H., 1998. Volcanism, tectonics, and stratigraphic correlations in Puerto Rico. In: Lidiak, E.G., Larue, D.K. (Eds.), Tectonics and Geochemistry of the Northeastern Caribbean. Geological Society of America Special Paper 322, Boulder, Colorado, pp. 1–34.

Jolly, W.T., Schellekens, J.H., Dickin, A.P., 2007. High-Mg andesites and related lavas from southwest Puerto Rico (greater antilles island arc): petrogenetic links with emplacement of the late cretaceous caribbean mantle plume. Lithos 98, 1–26. https://doi.org/10.1016/j.lithos.2007.01.011.

Keellings, D., Hernández Ayala, J.J., 2019. Extreme rainfall associated with Hurricane Maria over Puerto Rico and its connections to climate variability and change. Geophys. Res. Lett. 46, 2964–2973. https://doi.org/10.1029/2019GL082077.

Kroon, F.J., Schaffelke, B., Bartley, R., 2014. Informing policy to protect coastal coral reefs: insight from a global review of reducing agricultural pollution to coastal ecosystems. Mar. Pollut. Bull. 85, 33–41. https://doi.org/10.1016/j.marpolbul.2014.06.003.

Kumar, N., Ramirez-Ortiz, D., Solo-Gabriele, H.M., Treaster, J.B., Carrasquillo, O., Toborek, M., Deo, S., Klaus, J., Bachas, L.G., Whitall, D., Daunert, S., Szapocznik, J., 2016. Environmental PCBs in Guanica Bay, Puerto Rico: implications for community health. Environ. Sci. Pollut. Res. 23, 2003–2013. https://doi.org/10.1007/s11356-015-4913-9.

Larsen, M.C., Webb, R.M.T., 2009. Potential effects of runoff, fluvial sediment, and nutrient discharges on the coral reefs of Puerto Rico. J. Coast Res. 25, 189–208. https://doi.org/10.2112/07-0920.1.

Lidiak, E.G., Jolly, W.T., Dickin, A.P., 2011. Pre-arc basement complex and overlying early island arc strata, Southwestern Puerto Rico: overview, geologic evolution, and revised data bases. Geol. Acta 9, 273–287. https://doi.org/10.1344/105.000001715.

Lugo-Fernández, A., Hernandez-Avila, M.L., Roberts, H.H., 1994. Wave-energy distribution and hurricane effects on Margarita Reef, southwestern Puerto Rico. Coral Reefs 13, 21–32. https://doi.org/10.1007/BF00426431.

McLennan, S.M., 1989. Rare earth elements in sedimentary rocks: influence of provenance and sedimentary processes. In: Lipin, B.R., McKay, G.A. (Eds.), Rare Earth Elements. Mineralogical Society of America, Washington D.C., pp. 169–200

McLennan, S.M., Taylor, S.R., McCulloch, M.T., Maynard, J.B., 1990. Geochemical and Nd-Sr isotopic compositions of deep-sea turbidites: crustal evolution and plate tectonic associations. Geochem. Cosmochim. Acta 54, 2015–2050. https://doi.org/10.1016/0016-7037(90)90269-Q.

Mee, L., 2012. Between the devil and the deep blue sea: the coastal zone in an era of globalization. Estuar. Coast Shelf Sci. 96, 1–8. https://doi.org/10.1016/j.ecss.2010.02.013.

Meybeck, M., Vorosmarty, C., 2005. Fluvial filtering of land-to-ocean fluxes: from natural Holocene variations to Anthropocene. Compt. Rendus Geosci. 337, 107–123. https://doi.org/10.1016/j.crte.2004.09.016.

Miller, P.W., Kumar, A., Mote, T.L., Moraes, F.D.S., Mishra, D.R., 2018. Persistent hydrological consequences of hurricane Maria in Puerto Rico. Geophys. Res. Lett. 46, 1413–1422. https://doi.org/10.1029/2018GL081591.

Morelock, J., Schneidermann, N., Bryant, W.R., 1977. Shelf reefs, southwestern Puerto Rico. In: Frost, S.J., Weiss, M.P., Saunders, J.B. (Eds.), Reefs and Related Carbonates-Ecology and Sedimentology. American Association of Petroleum Geologists, Studies in Geology No. 4, pp. 17–25. Tulsa, Oklahoma.

Morrison, J.M., Goldhaber, M.B., Lee, L., Holloway, J.M., Wanty, R.B., Wolf, R.E., Ranville, J.F., 2009. A regional-scale study of chromium and nickel in soils of northern California, USA. Appl. Geochem. 24, 1500–1511. https://doi.org/10.1016/j.apgeochem.2009.04.027.

Newton, A., Carruthers, T.J.B., Icely, J., 2012. The coastal syndromes and hotspots on the coast. Estuar. Coast Shelf Sci. 96, 39–47. https://doi.org/10.1016/j.ecss.2011.07.012.

Orlando, J.L., Yee, S.H., 2017. Linking terrigenous sediment delivery to declines in coral reef ecosystem services. Estuar. Coast 40, 359–375. https://doi.org/10.1007/s12237-016-0167-0.

Orth, R.J., Marion, S.R., Moore, K.A., Wilcox, D.J., 2010. Eelgrass (*Zostera marina* L.) in the Chesapeake Bay region of mid-Atlantic coast of the USA: challenges in conservation and restoration. Estuar. Coast 33, 139–150. https://doi.org/10.1007/s12237-009-9234-0.

Otero, E., Carbery, K.K., 2005. Chlorophyll *a* and turbidity patterns over coral reefs systems of La Parguera Natural Reserve, Puerto Rico. Rev. Biol. Trop. 53 (Suppl. 1). https://www.scielo.sa.cr/scielo.php?script=sci_arttext&pid=S0034-77442005000300007. (Accessed 15 December 2020).

Pait, A.S., Whitall, D.R., Jeffrey, C.F.G., Caldow, C., Mason, A.L., Lauenstein, G.G., Christensen, J.D., 2008a. Chemical contamination in southwest Puerto Rico: an assessment of organic contaminants in nearshore sediments. Mar. Pollut. Bull. 56, 580–587. https://doi.org/10.1016/j.marpolbul.2007.11.007.

Pait, A.S., Whitall, D.R., Jeffrey, C.F.G., Caldow, C., Mason, A.L., Lauenstein, G.G., Christensen, J.D., 2008b. Chemical contamination in southwest Puerto Rico: an assessment of trace and major elements in nearshore sediments. Mar. Pollut. Bull. 56, 1953–1956. https://doi.org/10.1016/j.marpolbu1.2008.06.001.

Pittman, J., Armitage, D., 2016. Governance across the land-sea interface: a systematic review. Environ. Sci. Pol. 64, 9–17. https://doi.org/10.1016/j.envsci.2016.05.022.

Poleto, C., Merten, G.H., Minella, J.P., 2009. The identification of sediment sources in a small urban watershed in southern Brazil: an application of sediment fingerprinting. Environ. Technol. 30, 1145–1153. https://doi.org/10.1080/09593330903112154.

R Core Team, 2018. R: A Language and Environment for Statistical Computing. R Foundation for Statistical Computing, Vienna, Austria.

Ramos-Scharron, C.E., Torres-Pulliza, D., Hernandez-Delgado, E.A., 2015. Watershed- and island wide-scale land cover changes in Puerto Rico (1930s-2004) and their potential effects on coral reef ecosystems. Sci. Total Environ. 506, 241–251. https://doi.org/10.1016/j.scitotenv.2014.11.016.

Restrepo, J.D., Zapata, P., Diaz, J.M., Garzon-Ferreira, J., Garcia, C.B., 2006. Fluvial fluxes into the Caribbean Sea and their impact on coastal ecosystems: the Magdalena River, Colombia. Global Planet. Change 50, 33–49. https://doi.org/10.1016/j.gloplacha.2005.09.002.

Rogers, C.S., 1990. Responses of coral reefs and reef organisms to sedimentation. Mar. Ecol. Prog. Ser. 62, 185–202. https://doi.org/10.3354/meps062185.

Rosenbauer, R.J., Foxgrover, A.C., Hein, J.R., Swarzenski, P.W., 2013. A Sr-Nd isotopic study of sand-sized sediment provenance and transport for the San Francisco Bay coastal system. Mar. Geol. 345, 143–153. https://doi.org/10.1016/j.margeo.2013.01.002.

Ryan, K.E., Walsh, J.P., Corbett, D.R., Winter, A., 2008. A record of recent change in terrestrial sedimentation in a coral-reef environment, La Parguera, Puerto Rico: a response to coastal development? Mar. Pollut. Bull. 56, 1177–1183. https://doi.org/10.1016/j.marpolbul.2008.02.017.

Sherman, C., Hernandez, R., Hutchinson, Y., Whitall, D., 2013. Terrigenous sediment accumulation patterns at reefs adjacent to the Guánica Bay watershed. In: Whitall, D., Bauer, L.J., Sherman, C., Edwards, K., Mason, A., Pait, T., Caldow, C. (Eds.), Baseline Assessment of Guánica Bay, Puerto Rico in Support of Watershed Restoration. NOAA Technical Memorandum NOS NCCOS 176. Silver Spring, Maryland, USA, pp. 103–112.

Small, C., Nicholls, R.J., 2003. A global analysis of human settlement in coastal zones. J. Coast Res. 19, 584–599.

Smith, H.D., Maes, F., Stojanovic, T.A., Ballinger, R.D., 2011. The integration of land and marine spatial planning. J. Coast Conserv. 15, 291–303. https://doi.org/10.1007/s11852-0101-0098-z.

Spalding, M.D., McIvor, A.L., Beck, M.W., Koch, E.W., Möller, I., Reed, D.J., Rubinoff, P., Spencer, T., Tolhurst, T.J., Wamsley, T.V., van Wesenbeeck, B.K., Wolanski, E., Woodroffe, C.D., 2013. Coastal ecosystems: a critical element of risk reduction. Conserv. Lett. 7, 293–301. https://doi.org/10.1111/conl.12074.

Storlazzi, C.D., Field, M.E., Bothner, M.H., 2011. The use (and misuse) of sediment traps in coral reef environments: theory, observations, and suggested protocols. Coral Reefs 30, 23–38. https://doi.org/10.1007/s00338-010-0705-3.

Storlazzi, C.D., Field, M.E., Bothner, M.H., Presto, M.K., Draut, A.E., 2009. Sedimentation processes in a coral reef embayment: Hanalei Bay. Kauai. Mar. Geol. 264, 140–151. https://doi.org/10.1016/j.margeo.2009.05.002.

Storlazzi, C.D., Reguero, B.G., Cole, A.D., Lowe, E., Shope, J.B., Gibbs, A.E., Nickel, B.A., McCall, R.T., van Dongeren, A.R., Beck, M.W., 2019. Rigorously valuing the role of U.S. coral reefs in coastal hazard risk reduction. U.S. Geological Survey Open-File Report 2019- 1027, 42. https://doi.org/10.3133/ofr20191027.

Su, N., Yang, S., Guo, Y., Yue, W., Wang, X., Yin, P., Huang, X., 2017. Revisit of rare earth element fractionation during chemical weathering and river sediment transport. G-cubed 18, 935–955. https://doi.org/10.1002/2016GC006659.

Swain, D.L., Wing, O.E.J., Bates, P.D., Done, J.M., Johnson, K.A., Cameron, D.R., 2020. Increased flood exposure due to climate change and population growth in the United States. Earth's Future 8, e2020EF001778. https://doi.org/10.1029/2020EF001778.

Syvitski, J.P.M., Vorosmarty, C.J., Kettner, A.J., Green, P., 2005. Impact of humans on the flux of terrestrial sediment to the global coastal ocean. Science 308, 376–380. https://doi.org/10.1126/science.1109454.

Takesue, R.K., 2019. Geochemical and Isotopic Compositions of Stream Sediment, Parent Rock, and Nearshore Sediment from Southwest Puerto Rico, April 2017-June 2018. U.S. Geological Survey data release. https://doi.org/10.5066/P9QEAV6O.

Takesue, R.K., Storlazzi, C.D., 2017. Sources and dispersal of land-based runoff from small Hawaiian drainages to a coral reef: insights from geochemical signatures. Estuar. Coast Shelf Sci. 188, 69–80. https://doi.org/10.1016/j.ecss.2017.02.013.

Taylor, S.R., McLennan, S.M., 1985. The Continental Crust: its Composition and Evolution. Blackwell Science Publications, Oxford, p. 312.

Thrush, S.F., Hewitt, J.E., Cummings, V.J., Hatton, C., Lohrer, A., Norkko, A., 2004. Muddy waters: elevating sediment input to coastal and estuarine habitats. Front. Ecol. Environ. 2, 299–306. https://doi.org/10.1890/1540-9295(2004)002[0299:MWESIT]2.0.CO;2.

Trenberth, K., 2005. Uncertainty in hurricanes and global warming. Science 308, 1753–1754. https://doi.org/10.1126/science.1112551.

USGS, 2016. National Water Information System data available on the World Wide Web (USGS Water Data for the Nation) accessed October 20, 2019, at. https://waterdata.usgs.gov/nwis/dv?cb_00045=on&cb_00060=on&format=html&site_no=50126150&referred_module=sw.

van Veghel, M.L.J., 1994. Reproductive characteristics of the polymorphic Caribbean reef building coral *Montastrea annularis*. I. Gametogenesis and spawning behavior. Mar. Ecol. Prog. Ser. 109, 209–219.

van Woesik, R., Lacharmoise, F., Köksal, S., 2006. Annual cycles of solar insolation predict spawning times of Caribbean corals. Ecol. Lett. 9, 390–398. https://doi.org/10.1111/j.1461-0248.2006.00886.x.

Warne, A.G., Webb, R.M.T., Larsen, M.C., 2005. Water, Sediment, and Nutrient Discharge Characteristics of Rivers in Puerto Rico, and Their Potential Influence on Coral Reefs. U.S. Geological Survey Scientific Investigations Report 2005-5206, Reston, Virginia, p. 58.

Waterhouse, J., Brodie, J., Lewis, S., Audas, D.-m., 2016. Land-sea connectivity, ecohydrology and holistic management of the Great Barrier Reef and its catchments: time for a change. Ecohydrol. Hydrobiol. 16, 45–57. https://doi.org/10.1016/j.ecohyd.2015.08.005.

Weber, M., de Beer, D., Lott, C., Polerecky, L., Kohls, K., Abed, R.M.M., Ferdelman, T.G., Fabricius, K.E., 2012. Mechanisms of damage to corals exposed to sedimentation. Proc. Natl. Acad. Sci. U.S.A. 109, E1558–E1567. https://doi.org/10.1073/pnas.1100715109.

Weber, M., Lott, C., Fabricius, K.E., 2006. Sedimentation stress in a scleractinian coral exposed to terrestrial and marine sediments with contrasting physical, organic and geochemical properties. J. Exp. Mar. Biol. Ecol. 336, 18–32. https://doi.org/10.1016/j.jembe.2006.04.007.

Weiss, M.P., Goddard, D.A., 1977. Man's impact on coastal reefs- an example from Venezuela. In: Frost, S.J., Weiss, M.P., Saunders, J.B. (Eds.), Reefs and Related Carbonates- Ecology and Sedimentology. American Association of Petroleum Geologists, Studies in Geology No. 4, pp. 111–124. Tulsa, Oklahoma.

Whitall, D., Bauer, L.J., Sherman, C., Edwards, K., Mason, A., Pait, A., Caldow, C., 2013. Baseline Assessment of Guánica Bay, Puerto Rico in Support of Watershed Restoration. NOAA Technical Memorandum NOS NCCOS 176, Silver Springs, MD, p. 169.

Whitall, D., Mason, A., Pait, A., Brune, L., Fulton, M., Wirth, E., Vandiver, L., 2014. Organic and metal contamination in marine surface sediments of Guánica Bay, Puerto Rico. Mar. Pollut. Bull. 80, 293–301. https://doi.org/10.1016/j.marpolbul.2013.12.053.

Windom, H.L., Schropp, S.J., Calder, F.D., Ryan, J.D., Smith, R.G., Burnery, L.C., Lewis, F.G., Rawlinson, C.H., 1989. Natural trace metal concentrations in estuarine and coastal marine sediments of the southeastern United States. Environ. Sci. Technol. 23, 314–320. https://doi.org/10.1021/es00180a008.

Wolska, L., Mechlinska, A., Rogowska, J., Namiesnik, J., 2012. Sources and fate of PAHs and PCBs in the marine environment. Crit. Rev. Environ. Sci. Technol. 42, 1172–1189. https://doi.org/10.1080/10643389.2011.556546.

Wong, P.P., Losada, I.J., Gattuso, J.-P., Hinkel, J., Khattabi, A., McInnes, K.L., Saito, Y., Sallenger, A., 2014. Coastal systems and low-lying areas. In: Field, C.B., Barros, V.R., Dokken, D.J., Mach, K.J., Mastrandrea, M.D., Bilir, T.E., Chatterjee, M., Ebi, K.L., Estrada, Y.O., Genova, R.C., Girma, B., Kissel, E.S., Levy, A.N., MacCracken, S., Mastrandrea, P.R., White, L.L. (Eds.), Climate Change 2014: Impacts, Adaptation, and Vulnerability. Part A: Global and Sectoral Aspects. Contribution of Working Group II to the Fifth Assessment Report of the Intergovernmental Panel on Climate Change. Cambridge University Press, New York, pp. 361–409.

Yang, S.Y., Youn, J.S., 2007. Geochemical compositions and provenance discrimination of the central south Yellow Sea sediments. Mar. Geol. 243, 229–241. https://doi.org/10.1016/j.margeo.2007.05.001.